



DIE ERDE

Journal of the
Geographical Society
of Berlin

Mobile measurement techniques for local and micro-scale studies in urban and topo-climatology

Jochen Seidel¹, Gunnar Ketzler², Benjamin Bechtel³, Boris Thies⁴, Andreas Philipp⁵, Jürgen Böhner³,
Sebastian Egli⁴, Micha Eisele¹, Felix Herma¹, Thomas Langkamp³, Erik Petersen⁵, Timo Sachsen²,
Dirk Schlabling¹, Christoph Schneider⁶

¹ Institute for Modelling Hydraulic and Environmental Systems, Department of Hydrology and Geohydrology, University of Stuttgart, Pfaffenwaldring 61, 70569 Stuttgart, Germany, jochen.seidel@iws.uni-stuttgart.de, micha.eisele@iws.uni-stuttgart.de, felix.herma@iws.uni-stuttgart.de, dirk.schlabling@iws.uni-stuttgart.de

² Geographisches Institut, RWTH Aachen University, Wüllnerstr. 5b, 52056 Aachen, Germany, gunnar.ketzler@geo.rwth-aachen.de, timo.sachsen@geo.rwth-aachen

³ Institute of Geography, Center for Earth System Research and Sustainability, University of Hamburg, Bundesstr. 55, 20146 Hamburg, Germany, benjamin.bechteler@uni-hamburg.de, juergen.boehner@uni-hamburg.de, tom@tomblog.de

⁴ Laboratory for Climatology and Remote Sensing, Geographische Fakultät, Philipps-Universität Marburg, Deutschhausstr. 12, 35032 Marburg, Germany, boris.thies@geo.uni-marburg.de, sebastian.egli@geo.uni-marburg.de

⁵ Institute for Geography, University of Augsburg, Alter Postweg 118, 86159 Augsburg, Germany, andreas.philipp@geo.uni-augsburg.de, erik.petersen@student.uni-augsburg.de

⁶ Geography Department, Humboldt-Universität zu Berlin, Unter den Linden 6, 10099 Berlin, Germany, c.schneider@geo.hu-berlin.de

Manuscript submitted: 30 July 2015 / Accepted for publication: 23 September 2015 / Published online: 22 March 2016

Abstract

Technical development during the last two decades has brought new potential and new applications for mobile measurements. In this paper, we present six case studies where mobile measurement devices were used to acquire data for meteorological and climatological research. Three case studies deal with ground-based mobile measurements – on buses for urban climate measurements and on a vessel on a lake – and three with airborne platforms – on a cable car and on an unmanned aerial vehicle for vertical soundings and on a tethered balloon sonde for cloud physics. For each study, we describe the measurement set-up and address the potential and drawbacks of these applications. At the end, we discuss general aspects related to mobile observations especially concerning the time and space dimension of measurements.

Zusammenfassung

Die technischen Entwicklungen in den letzten zwei Dekaden haben neue Möglichkeiten für die mobile Messtechnik eröffnet. In diesem Artikel werden sechs Fallbeispiele vorgestellt, bei denen mobile Messungen für meteorologische und klimatologische Fragestellungen durchgeführt wurden. Drei dieser Fallbeispiele basieren auf bodengebundenen Messsystemen, die auf Bussen für stadtklimatologische Messungen bzw. auf einem Schiff installiert wurden. Bei den anderen drei Fallstudien kommen luftgestützte Messsysteme auf Seilbahnen, Fesselballons und Drohnen zum Einsatz. Für jedes Beispiel wird ein Überblick über die Geräte

Seidel, Jochen, Gunnar Ketzler, Benjamin Bechtel, Boris Thies, Andreas Philipp, Jürgen Böhner, Sebastian Egli, Micha Eisele, Felix Herma, Thomas Langkamp, Erik Petersen, Timo Sachsen, Dirk Schlabling and Christoph Schneider 2016: Mobile measurement techniques for local and micro-scale studies in urban and topo-climatology. – DIE ERDE 147 (1): 15-39



DOI: 10.12854/erde-147-2

und die Messtechnik gegeben und die Potentiale sowie Vor- und Nachteile erörtert. In einer abschließenden Diskussion werden allgemeine Aspekte mobiler Messungen adressiert, insbesondere hinsichtlich des Verhältnisses zwischen zeitlicher und räumlicher Dimension der Beobachtungen.

Keywords Mobile measurements, planetary boundary layer, urban climatology, atmospheric sounding, micro-scale climatology

1. Introduction

In climatology, mobile measurement techniques have been of great interest since the first investigations of this kind started more than 100 years ago with the first observations of the atmosphere using kites and balloons in several countries. However, in comparison to the technical development in remote sensing and ground-based energy flux and other measurements, mobile measurement techniques remained on a relatively poor standard for a long time. Partly, this may have been due to advanced modelling activities giving the impression of less need for detailed in situ measurements. However, during the last decade the need for a deeper understanding of processes behind spatial patterns has increased and is the subject of intense investigation to improve numerical models (TR 32 2015). Furthermore, the recent development of new technologies such as GPS, miniaturisation and wireless data transmission provide opportunities for new approaches in climate research. At the same time, the disadvantage of additional expenditure for the localization of all information and of poor accuracy due to reasons of lightweight equipment and spatial fuzziness is being reduced as new sensors with enhanced capabilities and accuracy as well as advanced data post processing procedures become more widely available. A new development in this context is e.g. the implementation of crowd sourcing (*Overeem et al. 2013*) and autonomous sensor networks. Presently, measurement techniques change rapidly resulting in installations which combine features from (multiple) micro-sensors including geopositioning and real-time data transmission in very small instruments. The new generation of instruments partly also integrates external processes like real-time data processing, assimilation into models and data visualization.

Measurement techniques are always related to atmospheric phenomena and their characteristic horizontal, vertical and time scales as discussed by *Oke (2006)* for the boundary layer as the systematic framework for urban and topo-climatology. Basic meteorological measurement systems do not cover these scales com-

pletely. Automatic weather stations (AWS) networks can capture process features at time scales of minutes or seconds, but they are designed to cover phenomena at meso- to macro-scale; the number of AWS required is a practical limitation for investigations at local to micro-scale. Meteorological towers and remote sensing instruments (e.g. SODAR) can provide data with high vertical and temporal resolution, but they are points in space and by far not applicable everywhere; radiosonde data are more widespread available but they have poor vertical resolution in relation to boundary-layer dimensions. Remote sensing is a very important 2D-data source, but can only cover some information on the earth's surface state and with limited temporal resolution. And sometimes these data sources are just not available, because a road is too busy for an AWS, a buoy network too costly for a certain investigation on a lake or a tower not available in the area of investigation or too small. However, although there is a variety of measuring techniques for boundary-layer investigations, a local or micro scale level is by far not reached as a whole and relevant processes are only partly captured. Many of the remaining data gaps in time and space can be filled with mobile measurement techniques.

In many fields of research mobile measurement techniques are the unique source of in situ data for local climate mapping with adequate temporal and spatial resolution. This is, for instance, the case in urban and topo-climatology to understand the small-scale structure of the urban heat island, local cold-air systems and other atmospheric characteristics near the ground. In urban climatology, early investigations focused on the overall urban effect at a scale of tens of kilometres, they were based on observations at very few fixed locations in and outside a greater city (e.g. *Howard 1833*). Later work aimed at analysing differences within cities at a horizontal scale of kilometres, more and more using – still slow – mobile instruments as in the studies of *Schmidt (1927, 1930)* and *Peppler (1929)*. Presently, effects of structures of hundreds of metres or less are subject to urban climate investigations, which is not simply a scaling factor of 10 but a scale transition from meso to local and micro-scale. In

this scale of investigation, effects and their classification have become a widely discussed recent cross-cutting issue. Such structures (“local climate zones”, LCZ) are typically those of blocks of houses; this is also the dimension of a source area or footprint a temperature sensor typically “sees” (Stewart and Oke 2012). For a statistical approach on structures of this scale, a mobile sensor system is an adequate measuring setup.

Measurements on water bodies are usually performed either by buoy weather stations or ship observations. Weather buoys typically form a station network at scales of hundreds of kilometres; ship observations are performed on a similar horizontal scale. While both measurements are commonly used on oceans, such systems are rarely in operation on small- to medium-scale lakes. For limnological research questions, measured data of the lake surface itself are required. For example, the internal circulation, which is responsible for the mixing process in lakes, is basically driven by the wind energy input into the lake surface. Therefore, knowledge of the wind distribution on the lake surface is very important and the unavailability of spatially heterogeneous wind fields limits detailed three-dimensional lake modelling (Wahl and Peeters 2014). This wind distribution is usually based on wind data from on-shore stations which implies that the distribution of the wind on the lake is not represented correctly by these measurements.

In the field of fog microphysics, Thoma et al. (2012) stated that especially the integration of measured fog droplet spectra over the fog layer would be necessary to properly simulate fog formation, dissipation and vertical fog extent. Unfortunately, there are almost no measurement data available concerning the vertical distribution of fog microphysics for the initialization of numerical models and to validate the theoretical liquid water content (LWC) profiles for satellite-based fog detection. In situ airborne measurements (Slingo et al. 1982; Hayasaka et al. 1995; Wang et al. 2009) are not permitted during ground fog situations. Measurements with towers have the problem that they often cannot capture the whole vertical fog profile (e.g. Fuzzi et al. 1992, 1998). However, balloon-borne systems with suitable sensors that allow for profiling fog microphysics are rare (Okita 1962; Pinnick et al. 1978).

Investigations on the structure of the boundary layer began on a vertical scale of hundreds of metres (e.g. de Fonvielle 1893). During the first half of the 20th century, radiosondes emerged and first routine observa-

tions were carried out with these instruments (DuBois et al. 2002). From the 1970s onwards, remote sensing techniques for the investigations of the boundary layer such as LIDAR (Light Detection and Ranging), SODAR (Sonic Detection and Ranging) and RASS (Radar Acoustic Sounding System) were developed (e.g. Wilczak et al. 1996), and nowadays these instruments are often used in combination for boundary-layer research (Emeis et al. 2008). Mobile airborne systems however provide direct measurements and allow for an enhanced vertical scale of analysis in special surroundings, e.g. on vertical gradients or for specific variables in connection with atmospheric physics. In classical boundary-layer investigations, a high vertical resolution can already be obtained and mobile instruments (e.g. on unmanned aerial vehicles) have the potential to provide an increased horizontal resolution from single points to land-use types in local or micro-scales. Using unmanned aerial vehicles (UAV) as a platform for meteorological and environmental measurements is a rather new, however well-established method by now, as indicated e.g. by regular meetings of the International Society for Atmospheric Research using Remotely piloted Aircraft (ISARRA). Besides professional platforms designed for heavy payload (often for remote sensing) and long-range flights, small and lightweight foam model aircrafts (fixedwing aircrafts) or multicopters (rotorcrafts) have proven to be a cost-effective and robust alternative if the sensors are of low or intermediate weight (Reuder et al. 2009; van den Kroonenberg et al. 2012; Reuder et al. 2012; Mayer et al. 2012; Salamí et al. 2014). While rotorcrafts are better suited for the examination in ultra-low levels, i.e. down to few metres and up to around 100 metres above ground level, fixed wing aircrafts can fly up to several kilometres (depending on the legal framework), offer flight durations up to one hour and more as well as high cruising speeds (e.g. 35 m s⁻¹). Thus these platforms offer new possibilities for the sounding of the atmospheric boundary layer.

In this paper we present six case studies where different mobile measurement systems and carrier platforms have been used in boundary-layer climatology. The aim is to demonstrate the potential of such mobile measurements in connection with access to climate data at smaller scales and to point out advantages and drawbacks of these systems. In Section 2, we present three case studies involving horizontal mobile ground-based measurements in cities and on lakes using buses and ships as carrier platforms. The two studies in Aachen and Hamburg address the investigation and develop-



Fig. 1 Combined temperature and GPS logger mounted on a public bus (reprinted from Buttstädt et al. 2011)

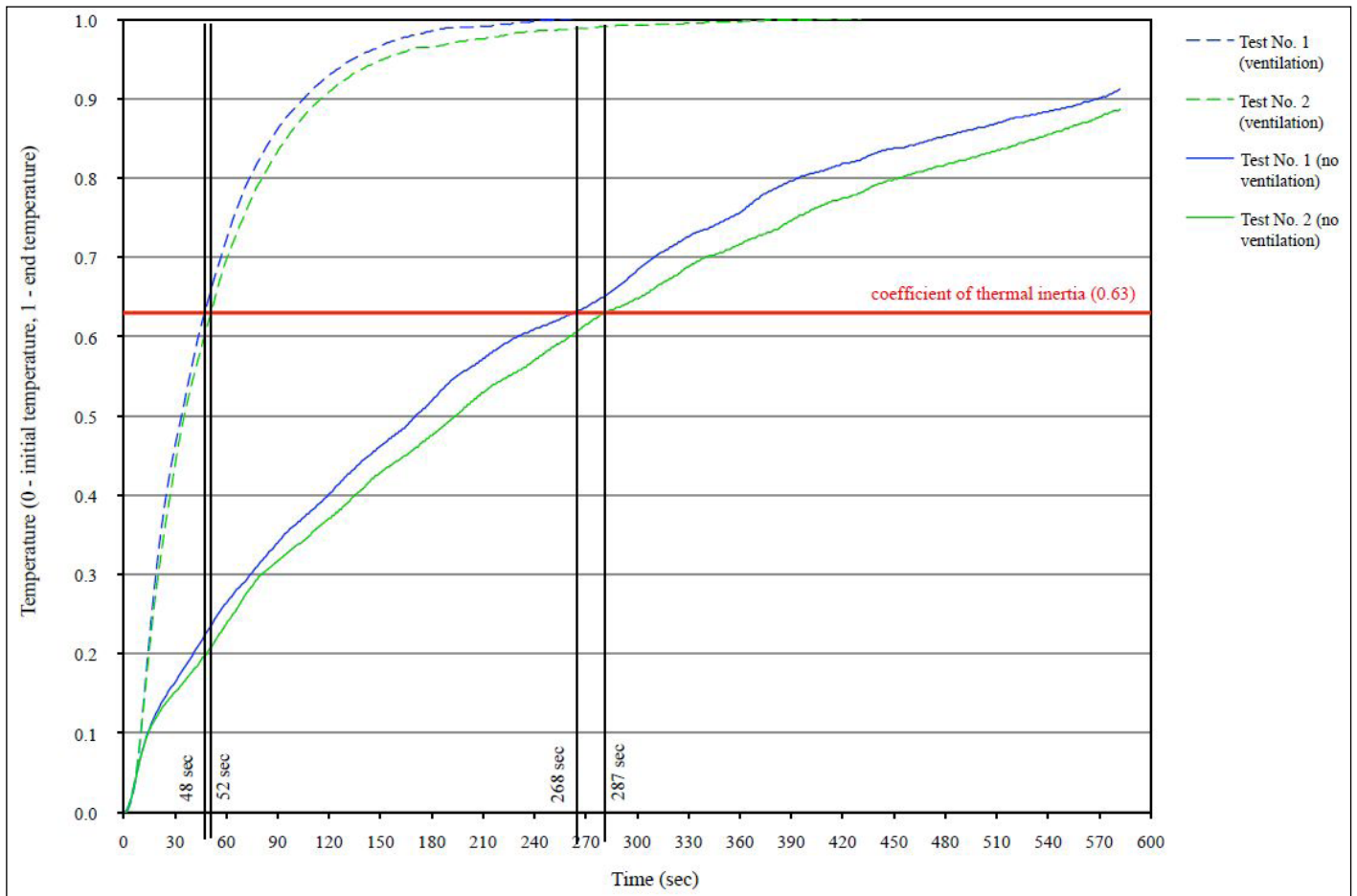


Fig. 2 Adaptation time of the thermometers in ventilated and non-ventilated state (reprinted from Buttstädt et al. 2011)

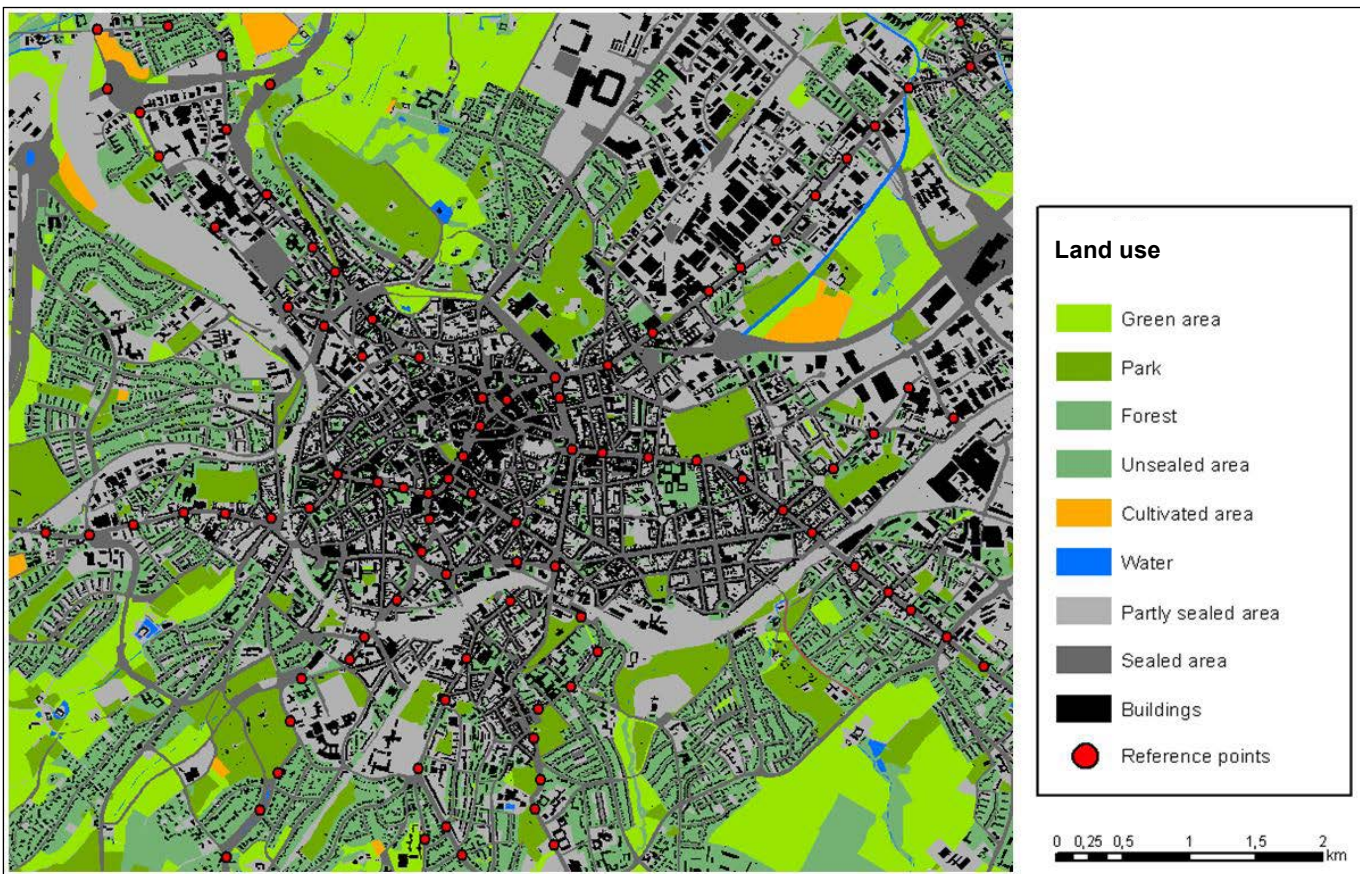


Fig. 3 Predefined points along bus tracks in Aachen (see also Buttstädt et al. 2011)

ment of the urban heat island. The third case study presents a mobile system for measuring wind on a lake. Section 3 deals with three case studies using airborne systems for the sounding of the lower planetary boundary layer. These are a system on a cable car, a tethered balloon system and a UAV for measuring meteorological variables and microphysical properties in the lower boundary layer. In Section 4 we summarize and discuss experiences with the different systems.

2. Ground-based horizontal soundings

2.1 Mobile urban climate measurements in Aachen

In two subsequent studies in Aachen, a concept for a mobile measurement platform for climate data near the ground with enhanced temporal and spatial data resolution and data analysis tools for applied urban climate studies was established. An overview of major preceding contributions on mobile measurements in urban climatology and a first design sketch of the system were presented in Buttstädt et al. (2011). Examples on data analysis of mobile

station data were given in Merbitz et al. (2012) and Buttstädt and Schneider (2014).

In the framework of the City2020+ project at RWTH Aachen University, a first experimental investigation was carried out using four pairs of small temperature and GPS loggers on public bus routes. The self-built measurement units were equipped with a radiation shield and mounted in the front part of the bus roof on the driver's side (Fig. 1).

First data sets were mainly used to analyze temperature and GPS logger properties in relation to the vehicle driving state (Buttstädt et al. 2011). One task in connection with the moving sensor platform was to transform the temporal sensor accuracy information into information on spatial resolution. To do so, the thermometer adaptation time, expressed by the time constant, was determined performing two tests with the results of 48 s and 52 s. Given the mean time constant value of 50 s and a vehicle speed of 5 ms^{-1} , which may be typical for an inner-urban situation, a spatial resolution of 250 m was achieved (Fig. 2). This matches with the dimensions of typical urban building structures like perimeter blocks.

Table 1 Regression model parameters for air temperature: afternoon situation; modified after Buttstädt and Schneider 2014

Input sequence	Parameter (radius)	Coeff.	Single R ²	Multiple R ²	RMSE
1	Altitude (A)	0.0123915	0.79 (-)		
2	> 90% sealing (250 m) (S90 ₂₅₀)	4.18342 · 10 ⁻⁴	0.51 (+)		
3	Green spaces (500 m) (G ₅₀₀)	8.0176 · 10 ⁻⁵	0.46 (-)		
4	Forest (500 m) (F ₅₀₀)	4.3349 · 10 ⁻⁵	0.21 (-)		
				0.82	0.38

Best fit equation (p < 0.05):

$$T = 2.29393 - 0.0123915 \cdot A + 4.18342 \cdot 10^{-4} \cdot S90_{250} - 8.017 \cdot 10^{-5} \cdot G_{500} - 4.3349 \cdot 10^{-5} \cdot F_{500}$$

Table 2 Regression model parameters for air temperature: evening situation; modified after Buttstädt and Schneider 2014

Input sequence	Parameter (radius)	Coeff.	Single R ²	Multiple R ²	RMSE
1	Buildings (500 m) (B ₅₀₀)	3.67743 · 10 ⁻⁴	0.73 (+)		
2	Altitude (A)	0.00447877	0.61 (-)		
3	Forest (500 m) (F ₅₀₀)	1.17895 · 10 ⁻⁴	0.35 (-)		
				0.80	0.35

Best fit equation (p < 0.05):

$$T = 2.7625 + 3.67743 \cdot 10^{-4} \cdot B_{500} - 0.00447877 \cdot A - 1.17895 \cdot F_{500}$$

Another task was to permanently evaluate the ventilation state of the sensor. The GPS signal was used to determine the driving speed and, thus, classify measured data as favourable or unfavourable if the threshold value of 5 m s⁻¹ was reached. This value is supposed to be sufficient for sensor ventilation. At the same time, this minimum speed keeps the duration of possible bus effects on the air very short, because the path lines from the vehicle front to the sensor are << 5 m and, thus, the exposure time is << 1 s.

The primary data processing concept was to transfer the temperature data into values relative to a nearby reference station. Afterwards, average values for certain time slots or street sections were calculated (Buttstädt et al. 2011). Additionally, temperature data were extracted for points along the bus route which leads to promising results especially in combination with air quality data from mobile measurements (Merbitz et al. 2012).

For purposes of urban climatology, an extended data processing concept based on predefined points was developed. For predefined points along the bus tracks, temperature and GPS data sets with a favourable driving state were extracted into a database (Fig. 3). At the

given speed of 5 m s⁻¹, these observations are expected to be located at least close to the predefined point (< 37.5 m). In an extensive study, data for 256 reference points along four bus tracks on 44 days between March 2010 and June 2011 were analysed in combination with land use information based on administrative GIS data (Buttstädt and Schneider 2014). A multiple regression model was set up which showed best correlation coefficients between temperature and land use data as proportions of green spaces, forest, areas of more than 90 % sealed surface, building density and altitude. The best multiple R² (0.82; Table 1) was obtained for green spaces and forest (both in 500 m radius), areas of more than 90 % sealed surface (in 250 m radius) and altitude for the afternoon situation and buildings and forest (both in 500 m radius) and altitude in the evening situation (R² = 0.80; Table 2).

These land-use characteristics are not only of statistical interest but also relevant for urban planning because they represent typical dimensions of urban land use. Thus, this multiple regression approach can also form the basis for applied urban climate studies. In connection with the climate change adaptation concept for the City of Aachen, a model for structure and extent of areas with thermal heat load was derived from the

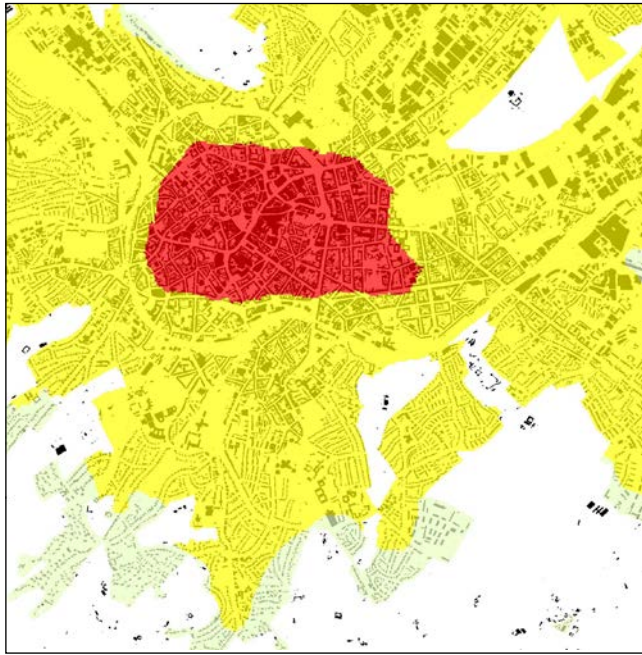


Fig. 4 Areas with thermal heat load in the city of Aachen, derived from a multiple regression approach. Built-up areas with high (red), medium (yellow) and low (green) heat load

above-mentioned multiple regression approach. This geostatistical model is based on the assumption that the temperature distribution, derived from the regression approach, can be applied on the whole area and can give an indication on areas with relatively high, medium and low thermal load. This subdivision was made using the temperature mean value plus and minus the standard deviation of all inner-urban model pixels (“high”, “medium”, “low heat load”; Fig. 4).

At present, a new sensor type “Urbmobi 2.0” has been developed. The main motivation for the concept of a new sensor is the lack of a combined climate and GPS sensor system, the limited accuracy of the former system and the demand for a sensor able to record data of multiple climate elements. This multi-sensor system with real-time data transmission and combined data base, modelling and visualization tools is a development within the Climate-KIC URBMOBI project (“Urban Mobile Instruments for Environmental Monitoring”). The sensor prototype was completed in 2014 and has passed several test runs (Fig. 5).

Urbmobi 2.0 collects temperature, humidity, solar radiation and GPS data and has been tested on cars and on public buses. The sensor data are saved on an SD card and additionally transmitted via GPRS to an external server. On the server, data is stored in a MySQL data base, auto-

matically checked for errors and analysed by detecting sensor environment information based on e.g. driving speed. Near-real-time modelling procedures couple the measured local data with regional meteorological model data to generate an urban climate model. An online visualization tool makes the measured and modelled data available in near-real-time. The additional sensors will give the opportunity to analyse more closely and quantitatively the spatial distribution of contributions by humidity and radiation as other important components of urban heat load. An urban climate investigation based on Urbmobi 2.0 data is in preparation.

Installing the sensor system on scheduled public service vehicles and extracting data for predefined points also allows for simulating an intra-urban cli-



Fig. 5 Urbmobi 2.0 sensor installed on a car



Fig. 6 Mobile measurement campaign in Hamburg. Left: Qstarz BT-Q1000XT GPS logger and Mobile Power Pack VT-PP-320b packed in the waterproof OtterBox 3000. Right: The instrumentation on the roof of a public transport bus. The logger is glued onto the OtterBox, the sensor is inside the radiation protection housing.

mate station network which will provide new opportunities for further urban climate research. Subsequently to the recent project phase, it is envisaged to develop a more complex multi-sensor device with additional air quality sensors for usage on different kinds of vehicles as permanently moving platforms.

2.2 Mobile urban climate measurements in Hamburg

The aim of the mobile measurement campaign in Hamburg was the collection of air temperature and relative humidity data within the urban area for urban heat island studies. Between 23 May and 29 October 2011, 15 public transportation buses were equipped with temperature and humidity sensors in cooperation with the Hochbahn Hamburg.

The loggers were selected according to the following requirements: a storage capacity of at least 100,000 measurements (≈ 6 d at 5 s logging frequency); small time constant to reach a spatial resolution of around 100 m despite the high speed of the bus platform of approximately 50 km h^{-1} within the city and up to 90 km h^{-1} on some roads; a waterproof and robust design against hot bus roofs and possible branch or hail beats; and an accuracy of $\pm 0.2 \text{ K}$ for air temperature and $\pm 2\%$ for relative humidity. These criteria were fulfilled by the DK311 logger, combined with the CO325 temperature sensor, respectively the RFT325 humidity sensor. The sensors were contained in a radiation protection housing and mounted on a custom

magnet holder. The position was recorded with Qstarz BT-Q1000XT Global Positioning System (GPS) loggers which were contained in a waterproof OtterBox 3000 and equipped with the additional VT-PP-320 power pack by Variotek. The GPS, temperature and humidity loggers were mounted magnetically on the front roof (see Fig. 6), where the temperature influence of the bus itself was found to be smallest (tested with surface temperature sensors at three positions of the roof). This set-up allowed for continuous measurements of up to six days (5-10 s intervals for temperature and humidity and 20 m for position and velocity). To minimize contamination by the roof temperature, which especially occurs at low travelling speeds, data collected at speeds below 12 km h^{-1} were removed during post-processing. Next, the temperature data were linearly interpolated to a frequency of 1 s and matched with the according time stamps of the GPS data. To reduce the size of the dataset, the measurements were subsequently averaged to one minute intervals and aggregated to a network of virtual stations with approximately 100 m spacing (derived from the centres of all measurements within a regular 100 m grid). This filtering resulted in more than 1 million observations which were stored in a PostgreSQL / PostGIS database.

For quality assessment, the aggregated mobile measurements were compared with observations from 25 stationary measurement sites from several data providers which are compiled in the Hamburg urban climate database (HUCDB) (Arnds et al. 2015). As criteria a maximal distance of 130 m and a maxi-

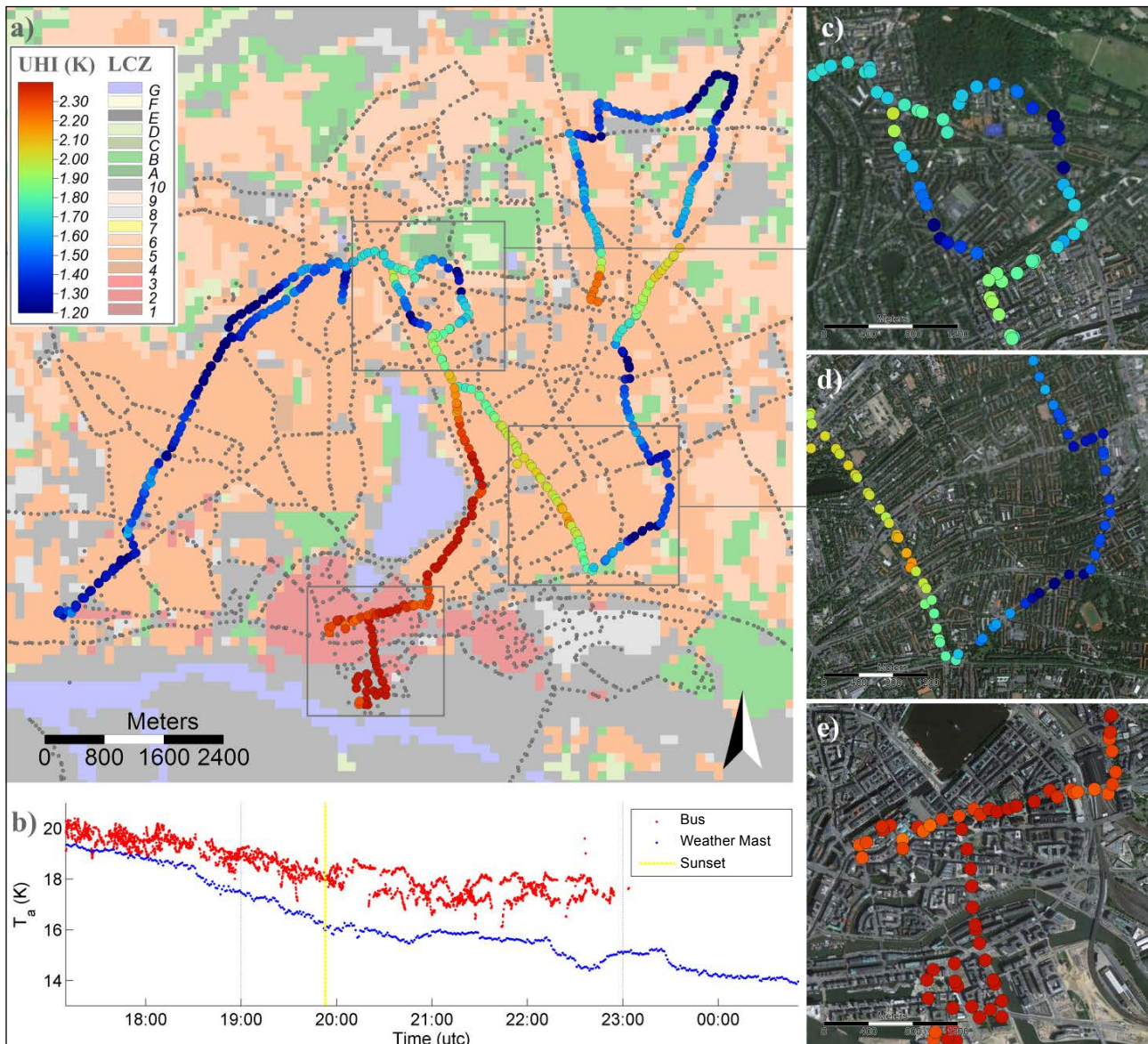


Fig. 7 Urban heat island for 21 June 2011. a) Spatial pattern recorded by buses and urban structures as Local Climate Zones (according to Bechtel et al. 2015). b) Time series of air temperatures measured by mobile devices on buses and reference station Hamburg Weather Mast. c-e) Examples of different urban structures and their thermal impact. Imagery: Google Earth.

mal absolute temporal deviation of 2.5 minutes were chosen which resulted in $n = 108$ available pairs for comparison. This resulted in a mean difference between stationary and mobile measurements of -0.15 K (standard deviation, $\sigma = 0.66$ K) and a mean absolute difference of 0.51 K ($\sigma = 0.44$ K).

Eventually, the urban heat island (UHI) intensity was calculated. It was defined as the difference of the temperature to stationary measurements from the Hamburg Weather Mast obtained by the Meteorological Institute of the University of Hamburg during the same minute (Brümmer et al. 2012). This high quality observation site

is above a vegetated surface (LCZ D) but since it is located close to the border of the built-up area it is likely that some urban influences could be advected. Nevertheless, we selected the Hamburg Weather Mast as reference station since it provides measurements every minute. Thus, the UHI intensity is defined according to Stewart and Oke (2012) as the difference between local climate zones rather than as urban-rural difference.

Figure 7 shows the UHI around sunset (21:53 CEST = 19:53 UTC) for the 21 June 2011 (21:00 UTC \pm 2 h). In the upper part the thermal differentiation within the city can be seen with a general temperature excess of

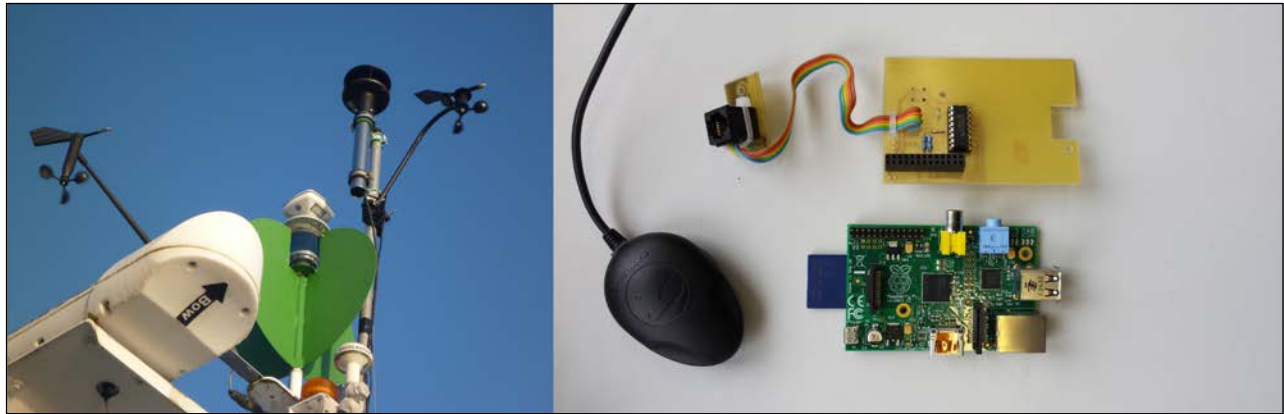


Fig. 8 Cup anemometer, wind vane and 2D ultrasonic anemometer (left) and RaspberryPi with A-D converter and GPS Tracker (right)

1.3-2 K and considerably higher values in the city centre, where the densest urban structures are located. Please be aware that the blue areas also show a UHI intensity of about 1.5 K. While the general pattern is plausible and mainly according to the urban structures in Hamburg (Bechtel 2011; Bechtel and Daneke 2012), it is superimposed by inter-calibration errors between the loggers as well as changing UHI conditions in the selected period, which complicates the interpretation. The latter can also be seen in the lower plot, where the observed air temperatures from the buses (red) and the reference station Weather Mast (blue) are displayed. It is clearly visible that the heat island already starts before sunset and the intensity increases with time. While the heat island intensity is largely similar before sunset, after sunset the bus measurements show a higher variation. This is related to spatial differences due to the movement of the buses within the urban structure and thus reflects different heat island magnitudes. Some fluctuations can also be seen in the reference data which themselves likely contain some urban effects.

The presented mobile measurement approach allows observations of the urban heat island with increased spatio-temporal coverage. However, the presented campaign also revealed some limitations. First, the spatial coverage was incomplete since in Hamburg the public buses are organized in several depots and for logistic reasons only specific lines could be equipped which did not leave the built-up area and mainly followed larger streets (see also Fig. 7) resulting in a reduced variance in temperature measurements. Since the UHI mainly occurs at night the temporal coverage due to the bus schedule is also not optimal. Further, the spatial air temperature differentiation is small compared to diurnal and seasonal differences, which

makes its detection difficult and places high requirements on the accuracy and inter-calibration of the loggers. Since the summer 2011 was rather humid and hence strong heat island conditions occurred only rarely, an additional mobile measurement campaign possibly with supplementary platforms such as taxis could complement the present findings.

2.3 Waterborne wind measurements – implementation of a single-board-computer-based system

The aim of this project was to implement a low-cost wind measurement system using a ship as carrier platform. Due to the ship's movement, the real wind velocity and direction have to be calculated from the apparent speed and direction by subtracting the ship's speed and course over ground. To plot the motion of the ship a GPS sensor was used. For wind measurement, a wind vane and a cup anemometer from a DAVIS Vantage Pro weather station were used which were calibrated against a Gill 2D ultrasonic anemometer yielding an R^2 of 0.992 (Fig. 8). GPS and wind data were processed and logged on the single-board-computer RaspberryPi (Fig. 8) which logged the measured raw data (2 s interval), calculated the real wind speed and direction and stored these variables as one-minute averages.

The measurement system was tested on Lake Constance on the "Kormoran" research vessel of the Institute of Lake Research (ISF) in Langenargen, Germany, during a routine operation on 23 September 2014. Figure 9 shows the boat speed over ground (blue), apparent wind (green) and corrected wind (red) plotted against time. The results show that the corrected wind speed does not depend on the speed of the ship.

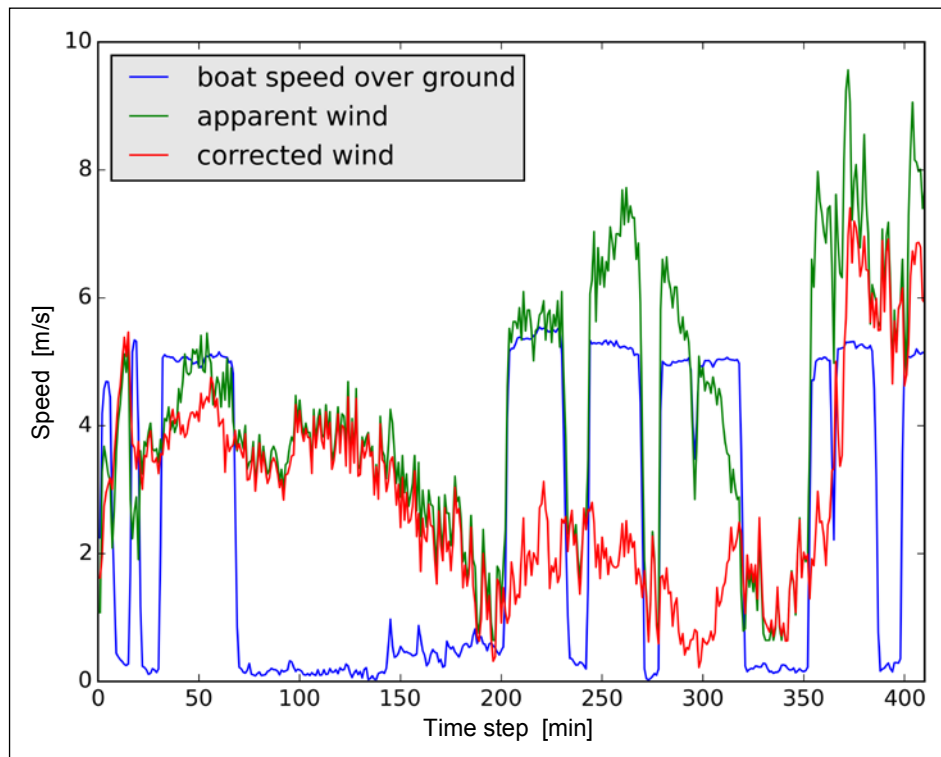


Fig. 9 Ship speed, apparent and corrected wind speeds on Lake Constance during the measurement campaign on 23 September 2014

For the correct wind direction, the course over ground of the ship needs to be determined. In the current system, the GPS tracker cannot detect a clear direction when the ship is not moving. This problem can be solved by an additional installation of a digital compass which will be implemented in the future. The rolling motion of the ship has an influence on the measured wind speed which was found during a previous test using a 3D ultrasonic anemometer and 3D accelerometer. We assume that this effect can be eliminated by averaging the data to intervals of at least 1 minute. This averaging can cause a positive bias, due to the quicker response of cup anemometers to acceleration than to deceleration. This causes the rotor to spin over-proportionally longer following a gust than the time from appearance of the gust to movement of the rotor (Kristensen 1998). Another issue is the deformation of the wind field (and subsequent measurement error) by the ship itself, which depends on the type of ship and may have anisotropic aerodynamic properties. For a first assessment of this influence, a direction-dependent correction factor could be determined by a comparison of ship and ground-based measurements, e.g. in a harbour. Another approach to deal with air-flow distortion is computational fluid dynamics modeling of the flow field, taking into account the three-dimensional geometry of the research vessel and its superstructure, as done by Griessbaum et al. (2010).

Due to the low costs of this system (≈ 250 €), the future plan is to equip several ferries on Lake Constance with such a wind measurement system in order to obtain more data on the spatial and temporal development of the wind field over the lake. Such data can be used as input for hydrodynamic lake modelling and to improve the simulation of the onshore wind. Furthermore, the measurement of other variables, such as temperature and rain, will be pursued through the installation of additional instruments.

3. Vertical sounding of the planetary boundary layer

3.1 Stability indices derived from atmospheric measurements on a cable car

The aim of this research work was to evaluate how temperature and humidity data can be used to determine small-scale vertical air stratification and whether tendencies for convective thunderstorm events can be detected.

The meteorological variables that were measured on the Predigtstuhl cable car at Bad Reichenhall, Germany, are atmospheric pressure, humidity and air temperature. The temperature and humidity sensor (Vaisala HMP 60) was installed in a radiation shield on a girder above the



Fig. 10 Cable car route (left), cable car cabin with sensor screen (centre) and GSM data logger with pressure sensor (right)

cable car cabin (Fig. 10). To reduce the time constant of the sensor, the protection cap was removed. The pressure sensor (Vaisala PBT 110), the data logger (R-Log) and the battery were installed inside the cabin. The data were transferred once per day via GSM. These data are used for the calculation of derived meteorological variables (e.g. lifting condensation level, specific humidity, vapour pressure, dew point temperature, etc.) which are relevant for atmospheric stratification and the subsequent calculation of stability indices. The vertical measurement range between the valley and the mountain station of the cable car is 1100 m. The height of the cable car above ground level varies from 5 to ≈ 200 m. The average speed of the cable car is 4.6 m s^{-1} . The altitude is calculated from the measured atmospheric pressure data with the barometric formula:

$$z_2 = -\frac{\ln \frac{p_1}{p_2} \cdot R_L \cdot T_m}{g} + z_1$$

where z_i is the elevation in m, p_i the atmospheric pressure in hPa, $R_L = 287 \text{ J kg}^{-1} \text{ K}^{-1}$ (the gas constant), $g = 9.81 \text{ m s}^{-2}$ (the gravitational acceleration) and T_m the mean temperature of the two calculation levels in Kelvin (Häckel 2008). A constant pressure indicates that the cable car is not moving. For the calculations, the initial pressure value always corresponds to the altitude of the valley or mountain station when the cable car starts or stops. This corrects for atmospheric air pressure changes over time. For further calculations just descents are considered since the data from the ascents are most likely influenced by the heat of the roof of the cabin when the cable car is at the valley

station which is exposed to the south. The first 100 and last 25 metres are discarded to eliminate boundary effects (e.g. warming during the stops, lower velocities while entering the station, etc.).

Different kinds of atmospheric layering (e.g. inversions, unstable conditions) and their development during the day can be seen in the data (Fig. 11), which are however limited by the operation time of the cable car between 8:00 and 16:00 CET. Furthermore, the number of runs during this time depends on the number of passengers and weather conditions, which is typical for recreational cable cars, but may differ at other localities that also provide commuter service.

The measured data from the cable car were used for the calculation of different kinds of stability indices. Several stability indices such as the Lifted Index (Galway 1956) or the Showalter Index (Showalter 1947) were investigated. Figure 12 shows the trend of the Showalter Index (SI) for a day with unstable atmospheric conditions. The red line defines the threshold value for a thunderstorm pre-warning. If the index value drops below the threshold a thunderstorm warning is to be issued.

Thus, threshold values for each stability index were established to distinguish stable and unstable atmospheric conditions. Firstly, the determination of threshold values was done with simple descriptive statistics like the median or quantiles of the data set. In a next step potential states for the occurrence of thunderstorms were determined by observations.

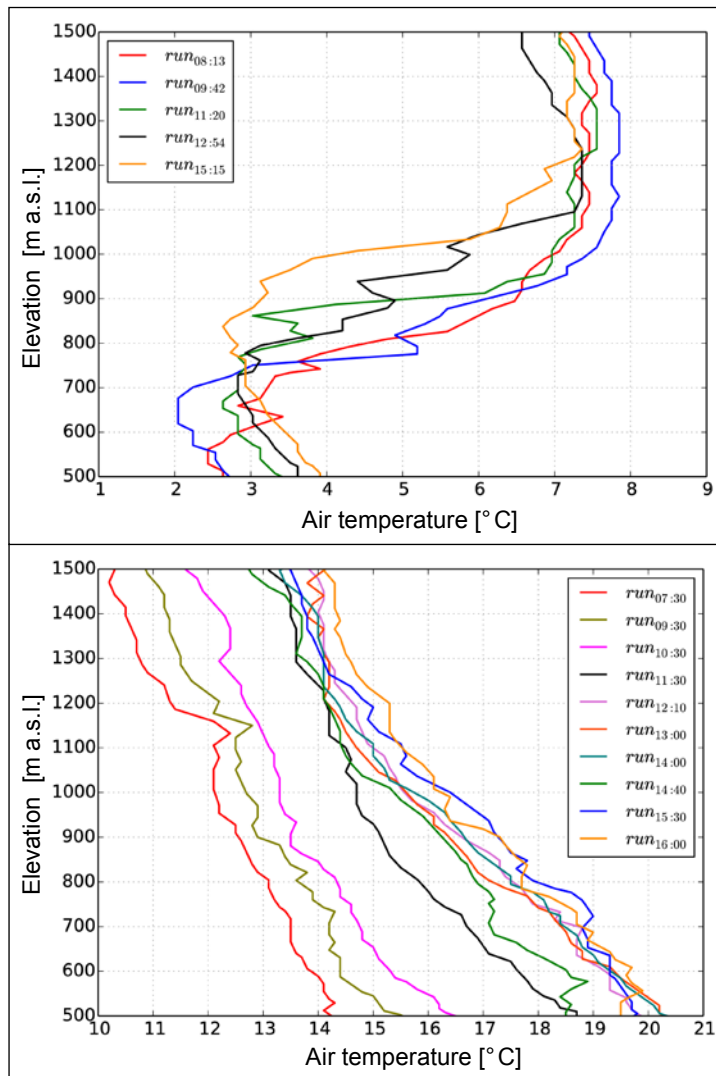


Fig. 11 Air temperature profiles with an inversion (top) and during neutral to unstable condition (bottom). The run index corresponds to the departure time of the cable car in CET.

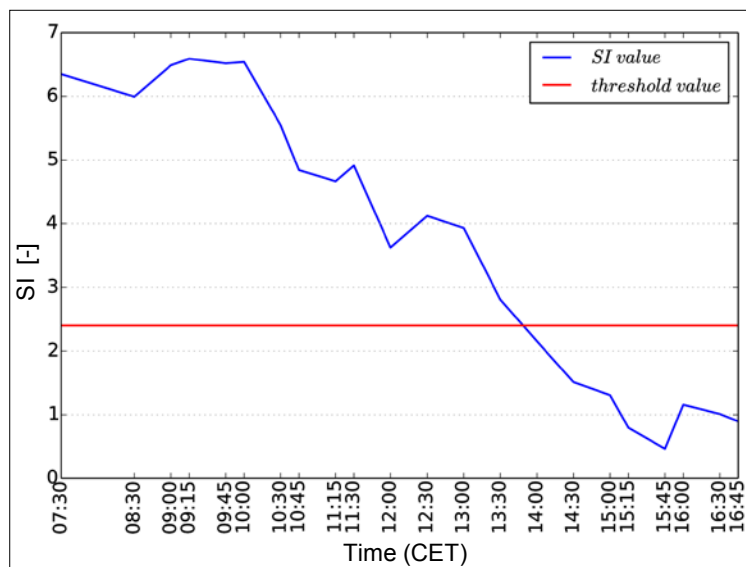


Fig. 12 Trend of the Showalter Index (SI) for 14 August 2011, a day with unstable atmospheric conditions

Table 3 Forecast verification with different skill scores for the Showalter Index (SI)

Skill scores	Config. I	Config. II	Range
Hit rate (HR)	0.58	0.79	[0, 1]
Probability of detection (POD)	0.78	0.66	[0, 1]
False alarm rate (FAR)	0.77	0.62	[0, 1]
Critical Success Index (CSI)	0.21	0.32	[0, 1]
Heidke Skill Score (HSS)	0.16	0.36	[-1, 1]
True Skill Statistics (TSS)	0.33	0.47	[-1, 1]

For this purpose, lightning maps, webcam images and observations of a ground weather station were considered. Accordingly, the time period three hours before an observed thunderstorm was assumed to be an unstable condition. The distinction between unstable and stable conditions enables the forecast verification by a skill score statistic where different quality criteria like the probability of detection, the false alarm ratio or the true skill statistics were investigated.

Table 3 shows the results of the forecast verification with different skill scores for the Showalter Index

(SI). The results of configuration I were established by considering only the stability index value as decision criterion. Configuration II includes meteorological observations like the atmospheric pressure, air and dew point temperature and absolute humidity of the ground weather station as additional criteria. Threshold values for the meteorological variables were determined like the index thresholds. This information was considered as a primary stage of a decision tree. If the first condition was not achieved, then the index was not considered anymore and no pre-warning was released.

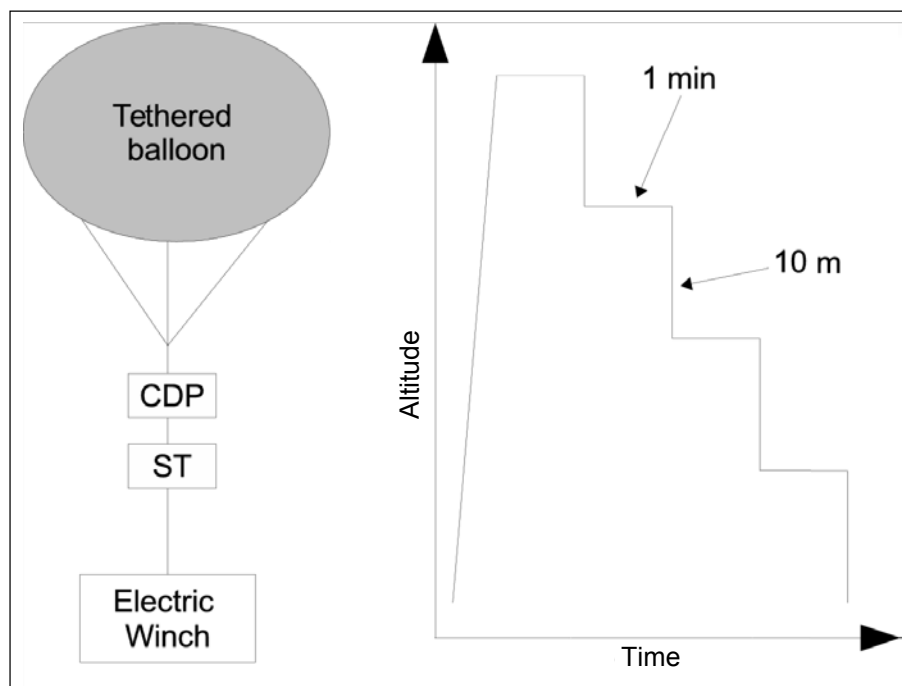


Fig. 13 Schematic illustration of the methodological set-up. CDP= Cloud Droplet Probe, ST= Smart Tether. Profiles were only measured during descents for 1 min on each 10 m level.

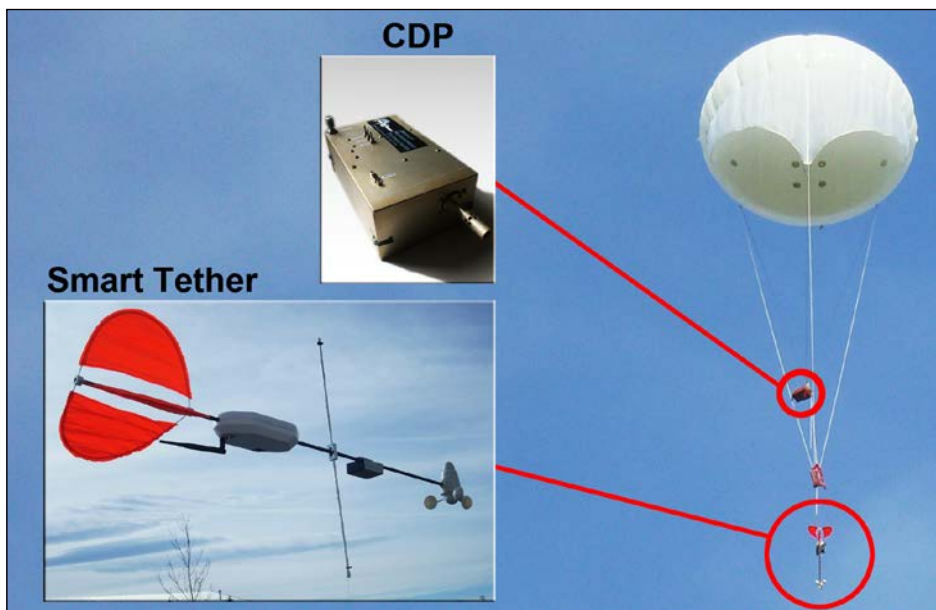


Fig. 14 The balloon-borne system during a test run

The forecast verification show for some skill scores, like the hit rate (HR) and the probability of detection (POD), promising results. Other scores like the false alarm rate (FAR) are unsatisfactory. The quality measures CSI, HSS and TSS are in an acceptable range. Certainly, the consideration of additional meteorological information improves the skill scores and thus the quality of the thunderstorm forecasts. These results are tentative and an extended investigation has to be done.

3.2 Measuring vertical distributions of microphysical properties in radiation fog

In the present study vertical profiles of microphysical properties were recorded during fog events by means of a newly designed tethered balloon-borne measurement system at the Marburg ground-truth and profiling station in Linden, Germany (Egli et al. 2015). The system is based on a composition of meteorological and microphysical instruments, including a novel optical particle counter.

Drop size distributions (DSD) are measured using a modified Cloud Droplet Probe (CDP) developed by Droplet Measurement Technologies, Inc., Boulder, CO, USA. The drop size distribution is measured at 30 intervals within the size range of 2 μm to 50 μm at a sampling frequency of 1 Hz. To analyse the vertical fog structure, liquid water content (LWC), droplet number concentration (Nt) and effective particle radius (re) were calculated from the recorded DSD

at each measurement height. Temperature, pressure, wind speed and relative humidity as well as the altitude of the instruments were measured with the wireless Smart Tether system distributed by Anasphere Inc., Bozeman, Montana, USA. In addition, altitude values were controlled with a barometric altimeter of a Garmin Oregon 450t GPS device.

Via controlled ascending to the fog top and incremental descending to the ground level, data profiles were recorded during the respective ground fog events. Ascent and descent of the measurement system were controlled with an electronic rope winch. A schematic illustration of the set-up and the measurement procedure is given in Figure 13. A photo of the instrumentation is depicted in Figure 14. To avoid a possible bias in the measurements due to drop expulsion in the lee of the balloon, only the data collected during the descents were used. The instruments were held for 1 minute at each altitude level and were sequentially lowered in steps of nominally 10 m. The intervals were suitable for an adequate representation of the drop size distribution at each measurement altitude while also guaranteeing a sufficient vertical resolution of the profile.

As an example, Figure 15 shows profiles of meteorological and microphysical variables on 29 October 2011. The temperature distribution (Fig. 15a) indicates the existence of a strong ground-touching inversion layer up to approx. 110 m. The humidity profile (Fig. 15b) shows a steep decline towards higher altitudes within the inversion layer which is in agree-

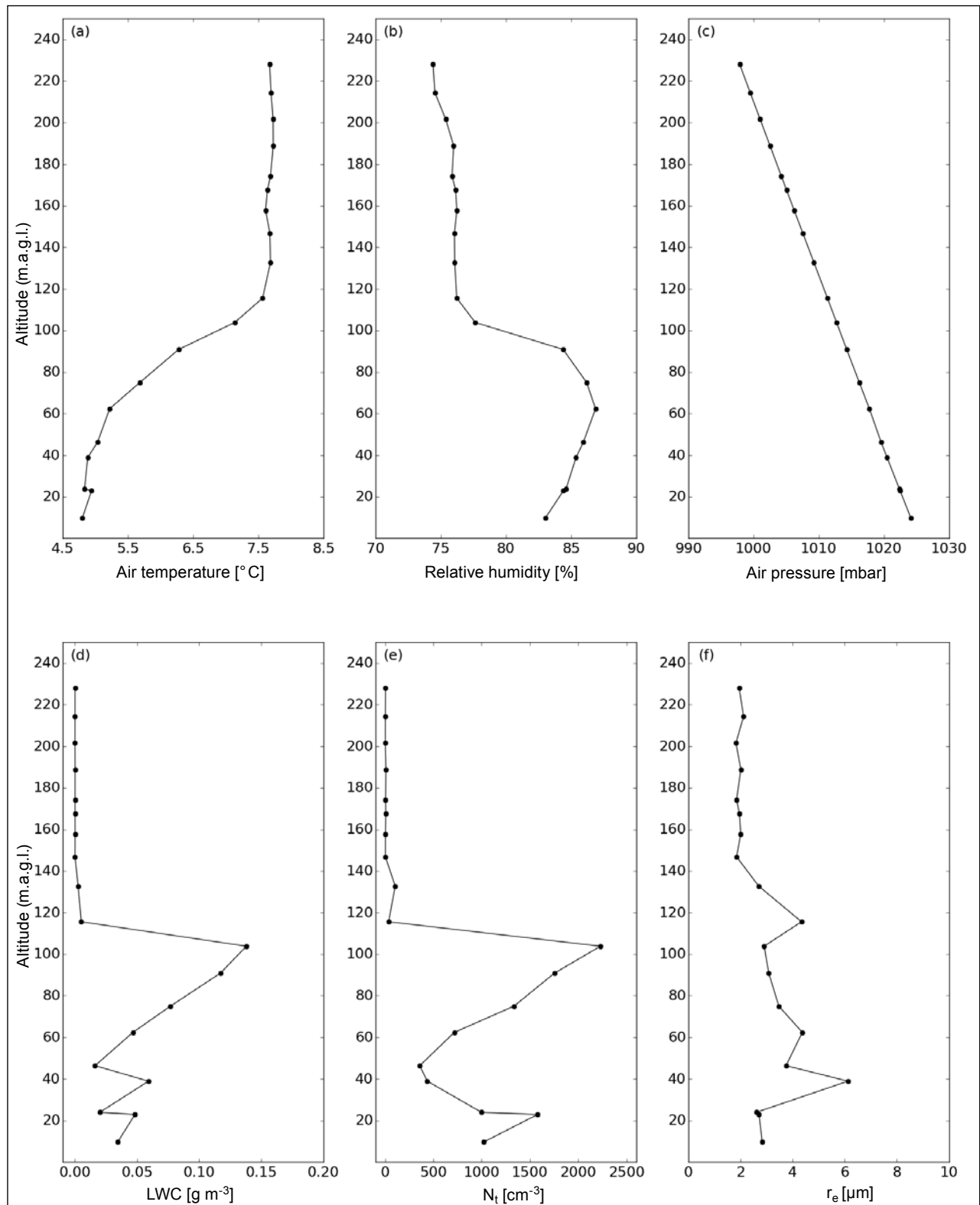


Fig. 15 Profiles of meteorological (a,b,c) and microphysical variables (d,e,f) measured between 04:16 and 04:37 UTC on 29 October 2011

ment to the temperature rise at these heights and indicates the interface of two different air masses, while air pressure values constantly decline over the whole profile (Fig. 15c). Concerning the microphysi-

cal variables, the absence of larger particles result in slightly lower LWC values (Fig. 15d) than in most other fog events measured during this campaign. The LWC values rise towards higher altitudes and reach

their maximum of 0.14 g m^{-3} at approx. 100 m height with small r_e (Fig. 15f) but high N_t values (Fig. 15e). Above, LWC values never exceed 0.01 g m^{-3} . This obviously can be attributed to the fact that the fog's top was exceeded for this part of the profile.

The introduced tethered balloon-borne system allows the measurement of fog microphysical and micrometeorological profiles with a high temporal and vertical resolution. A drawback of the system might be the required power supply for the electric winch and the helium for the balloon. Furthermore, human interaction during the measurements is needed. Thus, a continuous operation is not possible.

3.3 Unmanned aerial vehicles for meteorological sounding

In order to demonstrate the suitability of UAVs for exploring three-dimensional volumes of the boundary layer by in-situ measurements, a sounding ex-

periment retrieving four nearby vertical profiles by a single fixed wing UAV is described in the following section after a brief technical description. Since manual flight control is not capable of maintaining exact flight paths, only the hand start and landing is steered manually by a common radio control, while the sounding itself is operated by an autopilot controller. For meteorological measurements e.g. the APOGEE autopilot controller designed and published recently by ENAC (Ecole Nationale de l'Aviation Civile, France) is extremely useful as it integrates autonomous flight control, meteorological sensor operation and high-speed data recording on micro-SD cards in one single small and lightweight device driven by an STM32F405 processor. For navigation, an on-board inertial measurement unit and an on-board barometer is complemented by an external global navigation satellite system (GNSS) module. While there are plenty of suitable meteorological sensors, we confine here to address the Sensirion SHT75 temperature and humidity sensor. In order to omit radiation errors the

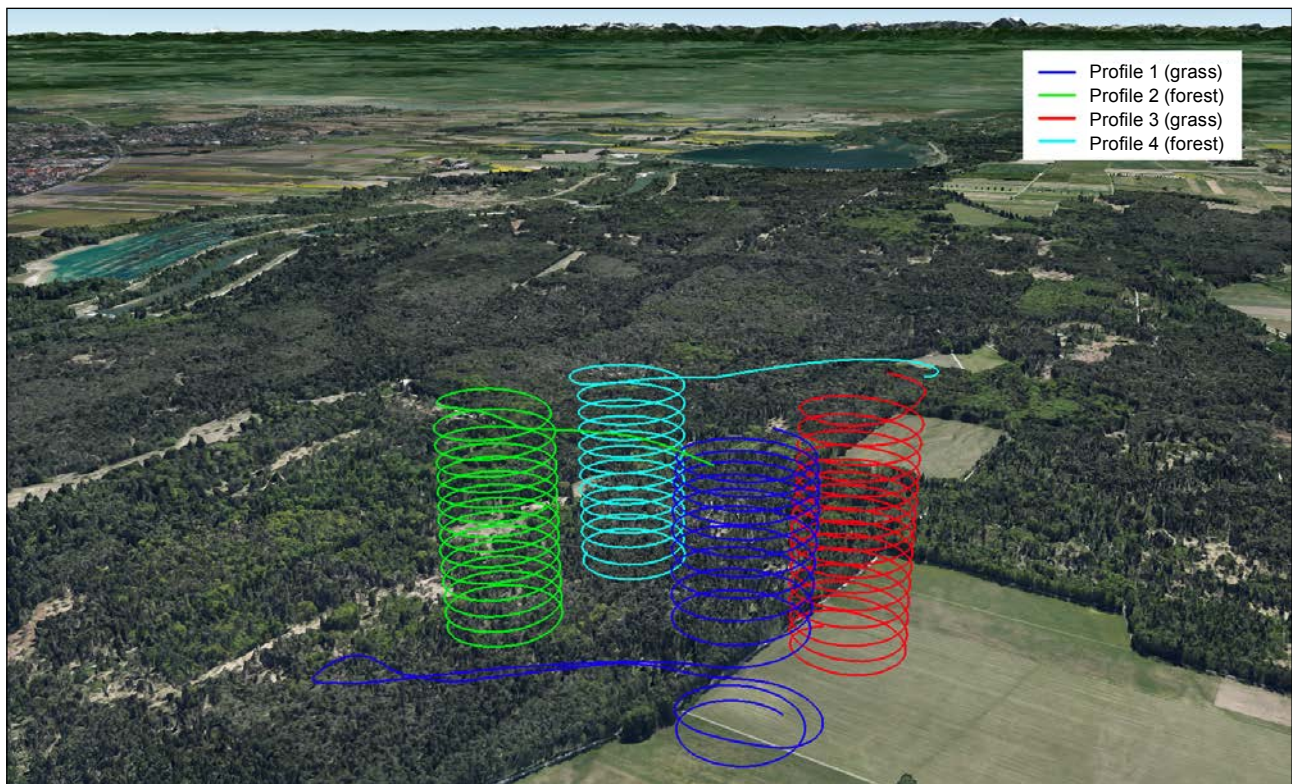
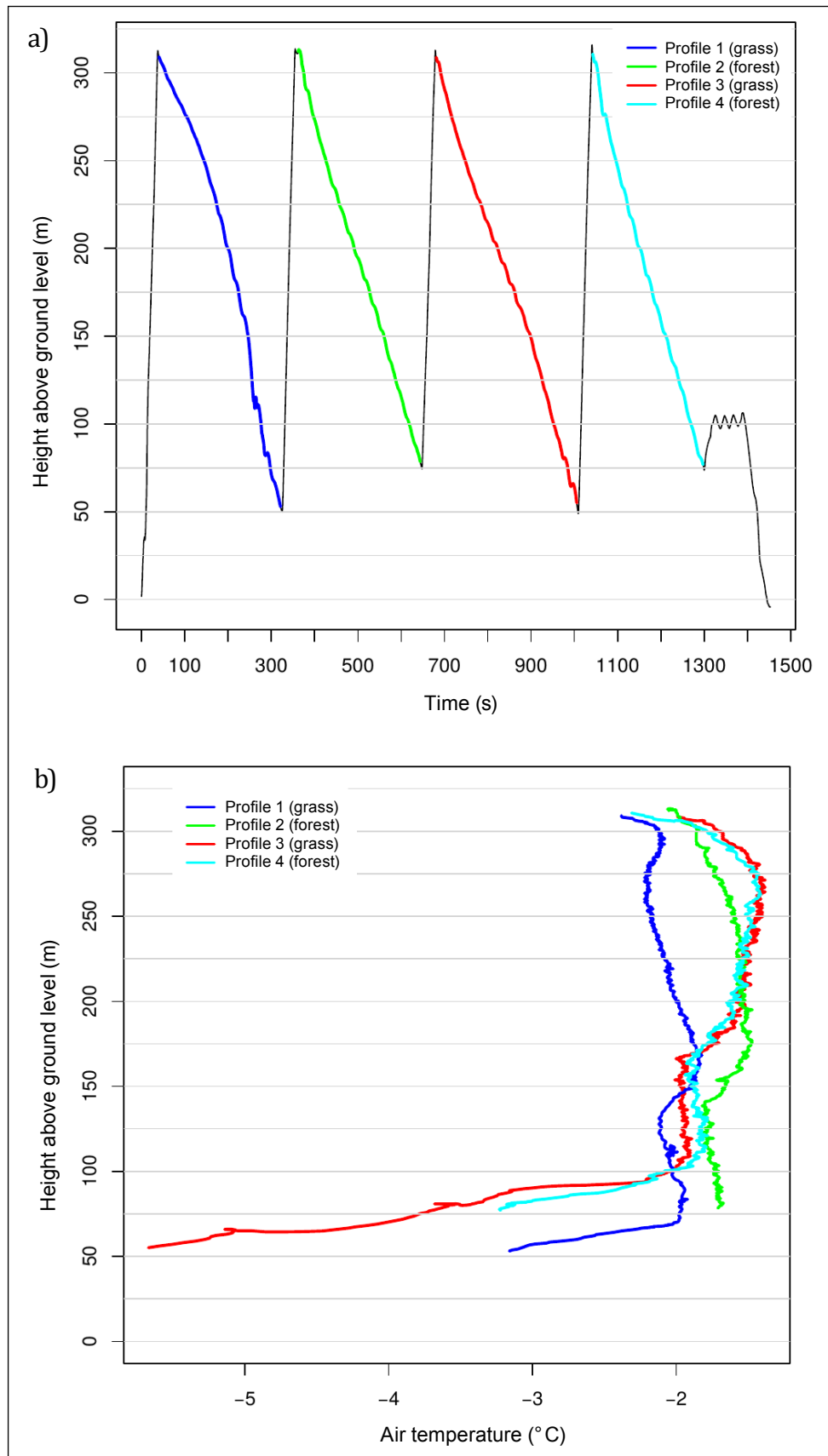


Fig. 16 Flight path as driven autonomously by an APOGEE autopilot controller (except takeoff, landing and the blue manually driven outlier loop) for the sounding experiment on 3 February 2015, comparing nearby temperature and humidity profiles over forest and grassland located at the Stadtwald Augsburg, Germany (river Lech and the Alpine range in the background viewing to south-east). Maximum height was 300 m above ground level. Sunrise was at 06:41 UTC, start and end of the downward helixes was from 06:38:32 to 06:43:19 UTC (blue helix), from 06:43:49 to 06:48:42 UTC (green helix), from 06:49:14 to 06:54:43 UTC (red helix) and from 06:55:15 to 06:59:34 UTC (cyan helix). Sources of map data: ©2015 Google, Digital Globe, GeoBasis-DE/BKG



sensor is mounted into a white plastic tube oriented into flight direction which ensures a ventilation of

at least 10 m s^{-1} airspeed (see e.g. Reuder et al. 2009). Programming of the autopilot controller including the

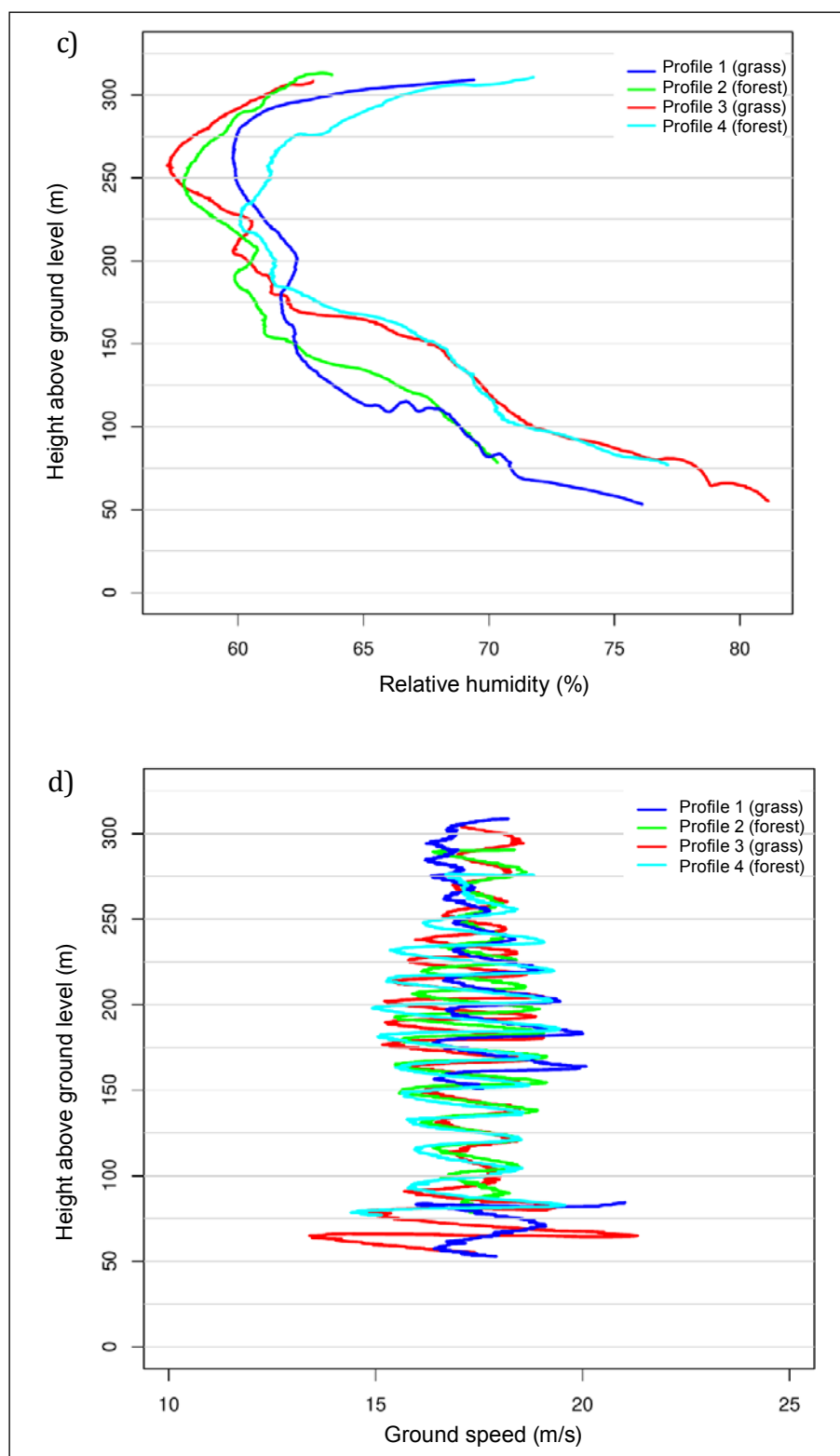


Fig. 17 Vertical profiles of the four helix flight paths (of Figure 16) of 3 February 2015 at 6:37 UTC: a) flight time versus altitude, b) temperature profile, c) relative humidity profile and d) UAV ground speed profile. The colours correspond to Figure 16. The gap in profile 1 results from the accidental non-orbital flight path at this height.

flight plan is done by the open-source software package PPRZ (<https://wiki.paparazziuav.org>). In order to

retrieve highly resolved profiles over a horizontally limited section of the surface the flight pattern of a

vertical helix is preferred. In the experiment using the flight path shown in *Figure 1* four helix profiles are retrieved with a horizontal distance of 300 m from each other in order to examine small-scale differences in the vertical structure of the lower boundary layer below 300 m above ground level. Since the SHT75 sensor needs around 3 seconds to adapt to the surrounding air, the steep high-speed climbing part of each profile is not used for interpretation but only the downward parts, where the UAV is gliding slowly down in circles with a flat pitch angle as shown in *Figure 16*.

The synoptic boundary conditions for the flight on 3 February 2015 led to nearly clear-sky conditions and wind speeds of around 1.5 m s^{-1} and less at a station located 3.5 km away for the whole night and morning. Additionally the whole area was covered with 5 cm of snow. The question under consideration was whether the land-use type of grass land on the one hand and forest on the other still plays a significant role in modifying the atmospheric boundary layer, under the given circumstances and at such small distances of a few hundred metres.

Figure 17a shows the height versus time in order to demonstrate the time lag of the three profiles which take ca. 5 minutes on average while the intermediate climbing to ≈ 300 metres above ground level takes around 30 seconds on average. Further on, the four temperature and relative humidity profiles are shown in *Figures 17b* and *17c*.

Concerning similarity between these profiles, there is no distinct correspondence between the two profiles over grass land (blue and red) or between the two profiles over the forest area (green and cyan). However, remarkable similarity can be found between the earlier (blue and green) profiles concerning temperature below ca. 100 m and humidity below ca. 175 m. Also the later (red and cyan) profiles show pronounced similarity concerning temperature throughout the profile and concerning humidity below 225 m.

Thus temporal differences clearly prevail over spatial differences and it can be concluded that the land-use type in this case is not relevant for any in-situ development of the air masses above 50 m from ground level. Thus temporal developments must be responsible for the observed differences, which may be caused by mainly two processes: direct in-situ effects of the changing radiation budget during sunrise, which took place during the blue profile flight or advection of air masses.

Regarding the temperature profiles (*Fig. 17b*) a strong surface inversion below 110 m above ground had developed over night and was captured by all four profiles except for the green one. A second, however weaker, upper level inversion layer is visible in all profiles between 130 and 200 m, lowest in the first (blue), higher in the second (green) and highest in the last two (red and cyan) profiles. Also the lower level inversion seems to climb over time (lowest for the first/blue and higher for the last/red and cyan profiles). This increase in altitude may be deduced to increasing incoming radiation and turbulence at sunrise. However this does not explain all differences. Instead, the temporal evolution of the temperature gives clear hints that advection of foreign air masses plays a significant role. Thus the second (green) temperature profile is around $0.3 \text{ }^\circ\text{C}$ warmer than the first (blue) one throughout the vertical distance, but the temporally following profiles (red and cyan) are cooler again (below ca. 200 m) which must be caused by advected air if vertical mixing can be excluded – which is the case here, due to the stable stratification. In the same manner the influence of advection can be observed for the relative humidity profiles above ca. 225 m (*Fig. 17c*).

In order to further address the question on the role of advection and wind, UAV ground speed recordings retrieved from the GNSS module, as shown in *Figure 17d*, may be used to characterize the wind conditions during the flight. This is possible because during the downward circles the propulsion of the UAV runs constantly with 30 % throttle and any change in ground speed during one cycle can be deduced to the effect of head wind and tail wind. Thus the amplitude of ground speed during one orbit reflects the absolute wind speed at this level. Regarding *Figure 17d* it becomes apparent, that indeed notable wind speeds occurred during the experiment. Thus there are ground speed amplitudes of at least around 1.5 m s^{-1} plus and minus the average throughout the profiles. Moreover, besides some strong anomalies at the lowest levels, there are distinctly higher wind speeds indicating a nocturnal low level jet between ca. 150 and 250 m, which advects the relatively warm and dry air masses mentioned above. Further on, an increase in altitude of the upper boundary of the jet layer can be observed which corresponds to the lifting of the upper level inversion in *Figure 17b*. However, in order to answer the initial question for this case study, it can be concluded that there are remarkable differences in the vertical structure of the boundary layer on such small scales, but that these differences are not induced by local differences

in surface cover, but may be ascribed mainly to advection and, concerning the increase in inversion heights, seemingly to the early morning increase in turbulence, which cannot be addressed in full detail here.

However, all in all, the four profiles, discussed in this case study, excellently demonstrate the considerable small-scale/short-term differences of the lower boundary layer and thus the importance of consulting not only one single profile for any further interpretation and application, e.g. for air quality questions. Further experiments may include larger spatial domains and more spiral profiles recorded with synchronous flights of not only one but a number of platforms. However, it has been demonstrated that the operation of small and cost-effective UAVs is already feasible and offers new possibilities in mobile in-situ measurements as a flexible alternative to remote sensing.

4. Summary and conclusion

The presented mobile measurement techniques and case studies have individual characteristics related to spatial coverage, specific carrier system, climate elements measured and data analysis (Tables 4 and 5). At present, most of these systems are set up for either horizontal or vertical measurements and for the climate elements temperature, humidity and wind. Only one of the systems is fully 3D-capable (UAV) and only one system has an extraordinary sensor (drop size). In all cases, the sensor systems were at least partly constructed by the investigation teams themselves.

Special effects of the sensor systems on the data make it necessary to define specific data evaluation or transformation procedures. Mobile measurement techniques with continuously moving sensors are associ-

Table 4 Overview of the horizontal mobile measurement systems

Section	2.1	2.2	2.3
Location	Aachen	Hamburg	Lake Constance
Carrier system	Buses/cars	Buses	Boat
Measured variables	Air temperature, location; additionally: humidity, solar radiation	Air temperature, humidity, location	Wind speed, wind direction, location
Frequency/temporal resolution	5 s	5-10 s	Raw data 2 s, processed data 1 minute
Horizontal resolution	250 m	≈100 m	Dependent on boat speed
Data logger	Hobo, own development "URBMOBI"	Driesen + Kern (DK 311)	Single board computer (RaspberryPi)

Table 5 Overview of the vertical mobile measurement systems

Section	3.1	3.2	3.3
Location	Bad Reichenhall	Marburg	Augsburg
Carrier system	Cable car	Tethered balloon	Unmanned aerial vehicle (UAV)
Measured variables	Air temperature, humidity, pressure	Drop size distribution, air temperature, pressure, humidity, wind speed, altitude	Air temperature, humidity, location, air speed, pressure
Frequency/temporal resolution	10 s	1 s	Position 4 Hz, airspeed 8 Hz, temperature and humidity 2 Hz
Vertical resolution	≈ 20 m	10 m	≈ 1 m
Vertical extent	1100 m	500 m	≈ 1000 m
Data logger	R-Log	Notebook	APOGEE SD-Card

ated with a specific transformation problem as a result of the permanent change of place. The fact that sensors are always subject to time constants leads to a temporal bias of the measurements ("response time"; Oke 2006). The data do not represent the current atmospheric conditions but a moving average value of the past adaptation time. For stationary measurements, averaging times considerably longer than the time constant will sufficiently reduce possible effects. For a continuously moving system of sensors subject to time constants, however, this leads to a specific spatial error based on the fact that speed is a relation between space and time. Thus, the temporal bias of a moving sensor system translates itself into a spatial bias. Additionally, moving platforms always have an internal spatial bias which is due to characteristics of the used GPS. In the case of wind measurements a special transformation of measured and platform speed and direction is necessary to obtain real wind speed and direction. In the case of the tethered balloon measurements the movement of the sensor system is stopped while performing individual measurements so that these transformation procedures are not necessary.

Another common characteristic of mobile measurement techniques is the unconventional sensor environment. Due to position and limits in size and weight, mobile sensors naturally do not meet the requirements of typical weather stations and, thus, there are specific requirements related to effects on instruments in urban environments (World Meteorological Organization 2008). Mobile sensors are additionally exposed to special technical installations of the moving platform, which easily can affect measurements. Consequently, the presented studies, in which this is of importance, discuss methods to minimize such effects. One focus is on using modified sensors like ventilated sensors. To do so, the platform speed information is used for data evaluation. In particular, a defined minimum speed near typical aspiration flow velocity forms the criterion for accepting or rejecting data. Future investigations on the use of mobile measurement techniques in climatology may especially target at enhanced knowledge on such effects. Overall the studies have demonstrated the large technical potential of mobile measurements. Especially, they allow for cost-effective observations with a spatially high resolution, which is not possible with stationary meteorological networks. Furthermore, the application is very flexible and location and time can be chosen to address relevant scientific questions. Some of the current shortcomings are likely to be eased by rapid technological development.

This does not only refer to ongoing miniaturization of sensors but also especially to the improvement of battery technology, which currently quite often limits the operational periods of mobile instrumentations.

Due to the present rapid development in sensor technology, a dynamic extension of the fields of climate-related applications is expected. In a few years, most of the current sensor types of previously large size or weight will be applicable on mobile platforms in miniaturized form. Thus, we will be able to observe significantly more details of small-scale structures of the earth's atmosphere in both space and time.

The main outcomes of the case studies on mobile measurement techniques and the perspectives of these techniques with respect to a deeper understanding of atmospheric processes can be summarized as follows. The ground-based sensor systems used on buses show to have a final spatial resolution of 250 m or less. This is possible due to the use of sensors with small time constants, relatively fast GPS positioning and passive ventilation. Thus, the provided air temperature data are not only of higher resolution but actually represent data of a smaller scale, i.e. local and even micro-scale. Such mobile systems, for the first time, give the opportunity for enhanced analysis of relations between different urban structures and climate near the ground within the scale of locale climate zones, which is no longer based on only a few AWS sites but on robust data quantities allowing for extended statistics. Beside some technical issues, like power supply and device size, the further development of this system will much depend on additional sensors and available carrier systems. In the special case of a mobile station on an inland water body, the scale and technical questions can be looked at as basically solved. A realization in scheduled inland lake ferry traffic is possible and the scientific task of providing local-scale meteorological input data for hydrological lake modelling is given. For the described mobile sensor systems, the perspective is even open to establish virtual station networks by continuously extracting data at defined sites which are frequently passed by regularly operating carrier systems.

The sensors used on the vertically operating carrier systems obtain data at different vertical resolution. The resolution of the cable car sensor system is comparable to existing tethered balloon instruments operating on a micro-scale and, thus, represents no improvement; the mobility of this system with classical sensors

is also restricted to a fixed vertical path. The great potential of this sensor concept consists in the existence of thousands of similar scheduled carrier systems in nearly all mountain areas of the world, where the benefits of data on atmospheric stratification for forecast and climatology are expected to be especially high and the data today can be accessed by GSM technique. The sensor system for microphysical properties in fog is mounted on a classical tethered balloon device. In this case, it is the sensor type which forms the novelty as a complicated optical particle counter now can be used in high vertical resolution and potentially in full 3D within a fog bank. This allows for a detailed analysis of the conditions of fog formation although the device has to be operated manually. Compared with these two systems, unmanned aerial vehicles as sensor platforms enable the logging of data in high vertical and horizontal resolution with partly automatable flight operation along free programmable flight paths. This implies a high potential for boundary-layer investigations. Restrictions are mainly the weight of sensors, limited power supply and security aspects.

Acknowledgements

'City 2020+' is funded by the Excellence Initiative of the German federal and state governments through the German Research Foundation (Deutsche Forschungsgemeinschaft, DFG).

URBMOBI was a project funded through the European Institute of Technology (EIT) Climate Knowledge and Innovation Centre (KIC). Within Climate-KIC the Urbmobi consortium is constituted by the Department of Geography of RWTH Aachen University, the Technical University of Budapest, TNO from the Netherlands, and two companies, ARIA from Paris, France and MEEO from Ferrara, Italy. We thank the Aachen public transport company ASEAG for cooperation and provision of their buses for mobile instrumentation in both the City2020+ and the URBMOBI projects.

We thank the Hamburg Hochbahn and especially *Thomas Blümel* for the fruitful cooperation and extensive logistic support with the bus measurements. Further, we thank *Daniela Arnds* and *Tobias Kawohl* who assisted in the measurement campaign. Further, we thank *Ingo Lange* and *Felix Ament* for the Weather Mast data. The Hamburg study was financed by the Cluster of Excellence CliSAP (EXC 177), University of Hamburg, funded through the German Science Foundation (DFG).

We thank *Bernd Wahl* and the Institute for Lake Research (ISF) in Langenargen for their support of the wind measurements on Lake Constance.

The study on the Predigtstuhl cabin car was carried out within the Project "Gekoppelte Verkehrs- und Hydrauliksimulation zur Steuerung von Verkehr bei Evakuierungsmaßnahmen (EvaSim)" funded by the German Federal Ministry of Education and Research. Furthermore, we thank the operators of the Predigtstuhlbahn in Bad Reichenhall for their cooperation.

The authors thank the German Research Foundation DFG for funding the project (BE1780/14-1; TH1531/1-1). The work is also part of the COST action EG Climet. The authors are also thankful to *Sebastian Achilles* for his support during the measurements.

Furthermore, the authors would also like to thank *Brigitte Lindauer* from the administrative district government of Swabia in Augsburg for the friendly permission to use the airspace over the conservation area Stadtwald Augsburg.

We are also grateful to two anonymous reviewers and to *Werner Eugster* who gave valuable comments to this paper.

References

- Arnds, D., J. Böhner* and *B. Bechtel* 2015: Spatio-temporal variance and meteorological drivers of the urban heat island in a maritime city. – *Theoretical and Applied Climatology*, online first, doi: 10.1007/s00704-015-1687-4
- Bechtel, B.* 2011: Multisensorale Fernerkundungsdaten zur mikroklimatischen Beschreibung und Klassifikation urbaner Strukturen. – *PFG Photogrammetrie, Fernerkundung, Geoinformation* 2011 (5): 325-338
- Bechtel, B.* and *C. Daneke* 2012: Classification of local climate zones based on multiple earth observation data. – *IEEE Journal of Selected Topics in Applied Earth Observations and Remote Sensing* 5 (4): 1191-1202
- Brümmer, B., I. Lange* and *H. Konow* 2012: Atmospheric boundary layer measurements at the 280 m high Hamburg weather mast 1995-2011: mean annual and diurnal cycles. – *Meteorologische Zeitschrift* 21 (4): 319-335
- Buttstädt, M., T. Sachsen, G. Ketzler, H. Merbitz* and *C. Schneider* 2011: A new approach for highly resolved air temperature measurements in urban areas. – *Atmospheric Measurement Techniques. Discussions* 4 (1): 1001-1019
- Buttstädt, M.* and *C. Schneider* 2014: Thermal load in a medium-sized European city using the example of Aachen, Germany. – *Erdkunde* 68 (2): 71-83
- de Fonvielle, W.* 1893: Thermometer soundings in the high atmosphere. – *Nature* 48: 160-161
- DuBois, J.L., R.P. Multhaupt* and *C.A. Ziegler* 2002: The invention and development of the radiosonde, with a catalog of upper-atmospheric telemetering probes in the National Museum of Ameri-

- can History, Smithsonian Institution. – Smithsonian Studies in History and Technology **53**. – Washington, D.C. 2002
- Egli, S., F. Maier, J. Bendix and B. Thies 2015: Vertical distribution of microphysical properties in radiation fogs – a case study. – Atmospheric Research **151** (1): 130-145
- Emeis, S., K. Schäfer and C. Münkel 2008: Surface-based remote sensing of the mixing-layer height – a review. – Meteorologische Zeitschrift **17** (5): 621-630
- Fuzzi, S., M.C. Facchini, G. Orsi, J.A. Lind, W. Wobrock, M. Kessel, R. Maser, W. Jaeschke, K.H. Enderle, B.G. Arends, A. Berner, I. Solly, C. Krusiz, G. Reischl, S. Pahl, U. Kaminski, P. Winkler, J.A. Ogren, K.J. Noone, A. Hallberg, H. Fierlinger-Oberlinninger, H. Puxbaum, A. Marzorati, H.-C. Hansson, A. Wiedensohler, I.B. Svenningsson, B.G. Martinsson, D. Schell and H.W. Georgii 1992: The Po valley fog experiment 1989. – Tellus B **44** (5): 448-468
- Fuzzi, S., P. Laj, L. Ricci, G. Orsi, J. Heintzenberg, M. Wendisch, B. Yuskiewicz, S. Mertes, D. Orsini, M. Schwanz, A. Wiedensohler, F. Stratmann, O.H. Berg, E. Swietlicki, G. Frank, B.G. Martinsson, A. Günther, J.P. Dierssen, D. Schell, W. Jaeschke, A. Berner, U. Dusek, Z. Galambos, C. Krusiz, N.S. Mesfin, W. Wobrock, B. Arends and H. Ten Brink 1998: Overview of the Po valley fog experiment 1994 (CHEMDROP). – Contributions to Atmospheric Physics **71** (1): 3-19
- Galway, J.G. 1956: The lifted index as a predictor of latent instability. – Bulletin of the American Meteorological Society **37**: 528-529
- Griessbaum, F., B.I. Moat, Y. Narita, M.J. Yelland, O. Klemm and M. Uematsu 2010: Uncertainties in wind speed dependent CO₂ transfer velocities due to airflow distortion at anemometer sites on ships. – Atmospheric Chemistry and Physics **10** (11): 5123-5133
- Häckel, H. 2008: Meteorologie. – 6. Auflage. – Stuttgart
- Hayasaka, T., T. Nakajima, Y. Fujiyoshi, Y. Ishizaka, T. Takeda and M. Tanaka 1995: Geometrical thickness, liquid water content, and radiative properties of stratocumulus clouds over the western North Pacific. – Journal of Applied Meteorology **34** (2): 460-470
- Howard, L. 1833: The climate of London deduced from meteorological observations made in the metropolis and at various places around it. – 2nd edition. – London
- Kristensen, L. 1998: Cup anemometer behavior in turbulent environments. – Journal of Atmospheric and Oceanic Technology **15** (1): 5-17
- Mayer, S., A. Sandvik, M.O. Jonassen and J. Reuder 2012: Atmospheric profiling with the UAS SUMO: a new perspective for the evaluation of fine-scale atmospheric models. – Meteorology and Atmospheric Physics **116** (1): 15-26
- Merbitz, H., M. Buttstädt, S. Michael, W. Dott and C. Schneider 2012: GIS-based identification of spatial variables enhancing heat and poor air quality in urban areas. – Applied Geography **33**: 94-106
- Oke, T.R. 2006: Towards better scientific communication in urban climate. – Theoretical and Applied Climatology **84** (1): 179-190
- Okita, T. 1962: Observations of the vertical structure of a stratus cloud and radiation fogs in relation to the mechanism of drizzle formation. – Tellus **14** (3): 310-322
- Overeem, A., J.C.R. Robinson, H. Leijnse, G.J. Steeneveld, B.K.P. Horn and R. Uijlenhoet 2013: Crowdsourcing urban air temperatures from smartphone battery temperatures. – Geophysical Research Letters **40** (15): 4081-4085
- Peppler, A. 1929: Das Auto als Hilfsmittel der Meteorologischen Forschung. – Wetter **46**: 305-308
- Pinnick, R.G., D.L. Hoihjelle, G. Fernandez, E.B. Stenmark, J.D. Lindberg, G.B. Hoidale and S.G. Jennings 1978: Vertical structure in atmospheric fog and haze and its effects on visible and infrared extinction. – Journal of the Atmospheric Sciences **35** (10): 2020-2032
- Reuder, J., M. Ablinger, H. Ágústsson, P. Brisset, S. Brynjólfsson, M. Garhammer, T. Jóhannesson, M. Jonassen, R. Kühnel, S. Lämmlein, T. de Lange, C. Lindenberg, S. Malardel, S. Mayer, M. Müller, H. Ólafsson, Ó. Rögnvaldsson, W. Schäper, T. Spengler, G. Zängl and J. Egger 2012: FLOHOF 2007: an overview of the mesoscale meteorological field campaign at Hofsjökull, Central Iceland. – Meteorology and Atmospheric Physics **116** (1-2): 1-13
- Reuder, J., P. Brisset, M. Jonassen, M. Müller and S. Mayer 2009: The small unmanned meteorological observer SUMO: A new tool for atmospheric boundary layer research. – Meteorologische Zeitschrift **18** (2): 141-147
- Salamí, E., C. Barrado and E. Pastor 2014: UAV flight experiments applied to the remote sensing of vegetated areas. – Remote Sensing **6** (11): 11051-11081
- Schmidt, W. 1927: Die Verteilung der Minimumtemperaturen in der Frostnacht des 12.5.1927 im Gemeindegebiet von Wien. – Fortschritte der Landwirtschaft. Zeitschrift und Zentralblatt für die gesamte Landwirtschaft **2** (21): 681-686
- Schmidt, W. 1930: Kleinklimatische Aufnahmen durch Temperaturfahrten. – Meteorologische Zeitschrift **47**: 92-106
- Showalter, A.K. 1947: A stability index for forecasting thunderstorms. – Bulletin of the American Meteorological Society **34**: 250-252
- Slingo, A., S. Nicholls and J. Schmetz 1982: Aircraft observations of marine stratocumulus during JASIN. – Quarterly Journal of the Royal Meteorological Society **108** (458): 833-856
- Stewart, I.D. and T.R. Oke 2012: Local climate zones for urban temperature studies. – Bulletin of the American Meteorological Society **93** (12): 1879-1900
- Thoma, C., W. Schneider, M. Masbou and A. Bott 2012: Integration of local observations into the one dimensional fog model PAFOG. – Pure and Applied Geophysics **169** (5): 881-893
- TR 32 2015: Why TR32? – Transregional Collaborative Research Centre 32. – Accessed online at: <http://tr32new>.

- uni-koeln.de/index.php/14-news/latest-news/8-why-tr32-news, 11/19/2015
- van den Kroonenberg, A.C., S. Martin, F. Beyrich and J. Bange* 2012: Spatially-averaged temperature structure parameter over a heterogeneous surface measured by an unmanned aerial vehicle. – *Boundary-Layer Meteorology* **142** (1): 55-77
- Wahl, B. and F. Peeters* 2014: Effect of climatic changes on stratification and deep-water renewal in Lake Constance assessed by sensitivity studies with a 3D hydrodynamic model. – *Limnology and Oceanography* **59** (3): 1035-1052
- Wang, J., P.H. Daum, S.S. Yum, Y. Liu, G.I. Senum, M.-L. Lu, J.H. Seinfeld and H. Jonsson* 2009: Observations of marine stratocumulus microphysics and implications for processes controlling droplet spectra: Results from the marine stratus/stratocumulus experiment. – *Journal of Geophysical Research* **114**: D18210
- Wilczak, J.M., E.E. Gossard, W.D. Neff and W.L. Eberhard* 1996: Ground-based remote sensing of the atmospheric boundary layer: 25 years of progress. – In: *Garratt, J.R. and P.A. Taylor* (eds.): *Boundary-layer meteorology. 25th anniversary volume, 1970-1995: Invited reviews and selected contributions to recognise Ted Munn's contribution as editor over the past 25 years.* – Dordrecht et al.: 321-349
- World Meteorological Organization 2008: *Guide to meteorological instruments and methods of observation.* – 7th edition. – World Meteorological Organization. – Geneva